Supplementary Information

Crystal facet-dependent Knoevenagel condensation of barium peroxide for saccharide upgrading

Rui Lu[a, *], Hao Chen [a, b], Han Yin [a, c], Xi Zhang [a, b], Songqing Lv [a], Xiangtao Kong [d], Fang Lu [a, *]

[a] Dalian Institute of Chemical Physics, Chinese Academy of Sciences, Dalian National Laboratory for Clean Energy, 457 Zhongshan Road, Dalian, 116023, China

[b] Henan Institute of Advanced Technology, Zhengzhou University, Zhengzhou, 450052, P. R. China

[c] University of Chinese Academy of Sciences, Beijing, 100049, China

[d] College of Chemistry and Chemical Engineering, Anyang Normal University, Anyang, 455000, China

*Corresponding authors: Rui Lu (lurui@dicp.ac.cn); Fang Lu (lufang@dicp.ac.cn)

Contents

1. Chemicals and Materials

All chemicals were of analytical grade and used as received unless otherwise indicated. D-Glucose (AR), barium hydroxide octahydrate (≥98.0%), absolute methanol (≥99.7%) and absolute ethanol (≥99.7%) were purchased from Shanghai Chemical Reagent, Inc. of the Chinese Medicine Group. Acetylacetone (≥99.5%), isopropanol (≥99.7%), magnesium oxide (≥98.0%), calcium oxide (97%), barium carbonate (≥99.0%), sodium hydroxide (AR) and anhydrous sodium carbonate (≥99.8%) were provided by Tianjin Kemiou Chemical Reagent Co. Ltd.. Barium oxide (B104893, 99.95%), barium peroxide (B299364, AR), D-mannose (M103969, 99.0%), D-galactose (98%), D-xylose (X101009, 98%) and D-maltose monohydrate (M104815, 97%) were purchased from Shanghai Aladdin Biochemical Technology Co., Ltd.. Barium Acetate (B802117, 99%) was purchased from Macklin Reagent Co. Ltd.. Maleic acid (M0006, >99.0%) was purchased from Tokyo Chemical Industry Co., Ltd.. Deuterium oxide was provided by Cambridge Isotope Laboratories, Inc.. High pure gases were provided by the gas reservoir of Dalian Institute of Chemical Physics.

2. Characterizations of FT-IR spectra and electron microscope
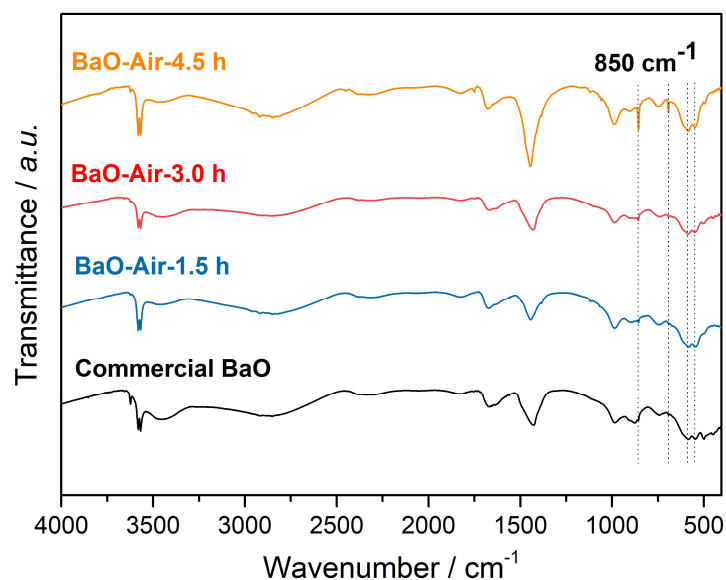
Fig. S1 FT-IR spectra of commercial BaO and BaO calcinated under static air for different times

The results of FT-IR characterization were shown in Fig. S1. The broad peaks at 585 cm^{-1} and 550 cm^{-1} were assigned to the vibration of Ba-O bond. Compared to commercial BaO, the calcinated BaO sample under static air appeared a new peak of 850 cm^{-1} which was assigned to the stretching vibration of the peroxyl (O-O) bond. Moreover, the peak intensity of peroxide bond increased gradually with the prolonging of calcination time.
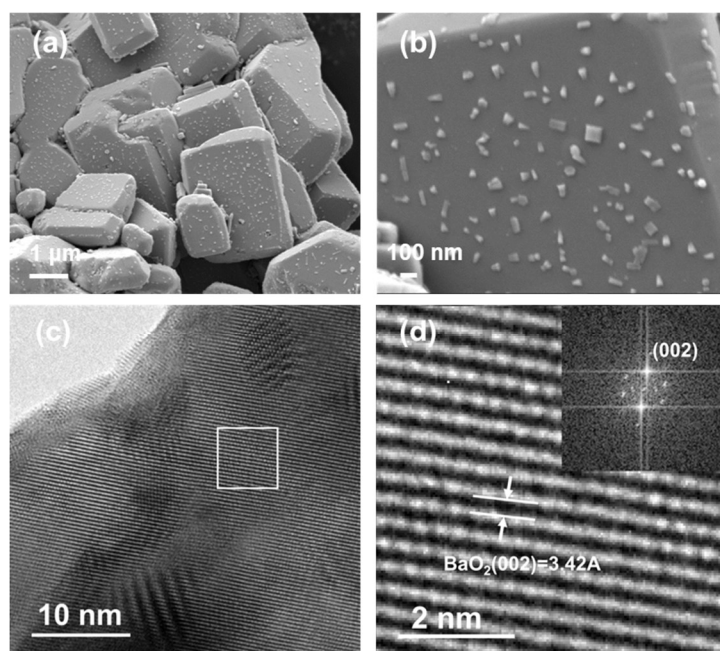
Fig. S2 Scanning electron microscope (SEM) images (a, b) and transmission electron microscope (TEM) images (c, d) of commercial BaO_2

As shown in Fig. S2a and S2b, commercial BaO_2 had the relatively regular micrometer-sized block structure, with multiple sharp-edged squares accumulating together. There were also many nanometer-sized structures on the surface of the micrometer-sized block structure. In the TEM images (Fig. 2c and 2d), the crystal facet (002) with a lattice spacing of 3.42 Å dominated.

3. Measurement of the base strength and basic site amounts of solid bases by Hammett indicator and titration methods

The melting phenomenon of BaO would occur as calcinated above 450 °C in the air atmosphere, and it was difficult to analyze the alkaline properties of the sample by the CO_2 temperature programmed desorption (CO_2-TPD). The Hammett indicator and titration methods were applied to measure the base strength and amounts of basic sites of various alkali earth metal oxides according to the references.[1,2] And the detailed procedures for determining base strength and amounts of basic sites were described as follows, respectively.

The pre-dried sample (50 mg) was weighed and transferred into a glass test tube and 5 mL of dried benzene was added. The mixture was dispersed evenly by ultrasonic treatment for 30 min. The Hammett indicators were dissolved in benzene to form a 0.1% solution which was added to the sample solution dropwise (two drops). The test tube was ultrasonic treated to accelerate the adsorption equilibrium of the indicator on the sample surface. After the adsorption equilibrium was reached, the indicator changed from acidic color to alkaline color, indicating that the basic strength of the sample was greater than that of the indicator.

Benzoic acid was dissolved in benzene to form a 0.05 mol·L^{-1} solution. The pre-dried sample was weighed and transferred into a glass test tube followed by titrated with the above benzoic acid solution. The change of the color of the sample surface from the alkaline color of the indicator to the acidic color was the end point of titration. The amounts of basic sites of the sample were calculated according to the consumption of benzoic acid, and the calculation formula was as follows.

$$\text{Amounts of basic site} = \frac{\text{Consumption of benzoic acid}}{\text{Mass of sample}}$$

As shown in Table S1, the H_- scales of basic sites on all tested samples were within the range of $9.3 < H_- < 15.0$ which indicated that their base strength might exist at similar level. Meanwhile, the amounts of basic sites increased with atomic numbers and the order was MgO < CaO < BaO which was consistent with that of the conversion of glucose in Table S2. It's worth noting that the amounts of basic sites of BaO before and after calcination in air were 0.55 and 0.62 mmol·g^{-1}, respectively. The calcination procedure only increased the number of basic sites of BaO slightly. Moreover, the number of basic sites of commercial BaO$_2$ was 0.26 mmol·g^{-1}, and the calcination in nitrogen caused the value to drop to 0.20 mmol·g^{-1}.

Table S1 Base strength and amounts of basic sites of various alkali earth metal oxides determined by Hammett indicator and titration method.

Entry	Solid base	Base strength (H_-)	Amounts of basic site (mmol·g^{-1})
1	MgO	$9.3 < H_- < 15.0$	0.25
2	CaO	$9.3 < H_- < 15.0$	0.35
3	BaO	$9.3 < H_- < 15.0$	0.55
4	BaO-Air-4.5h	$9.3 < H_- < 15.0$	0.62
5	BaO$_2$	$9.3 < H_- < 15.0$	0.26
6	BaO$_2$-N$_2$-2.0h	$9.3 < H_- < 15.0$	0.20

4. Reaction performance of the alkaline earth metal oxides

Table S2. Reaction performance of the alkaline earth metal oxide on the condensation reaction of glucose and acetylacetone [a]

Entry	Solid base	Calcination atmosphere	Conversion of glucose /%	Yield of C-glucoside ketone /%
1	Blank	-	0.0	0.0
2	MgO	Nitrogen	13.4	0.0
3	CaO	Nitrogen	93.0	30.4
4	BaO	Nitrogen	>99.9	36.1
5[b]	BaO	Nitrogen	>99.9	39.8
6[b,c]	BaO	Air	>99.9	77.0

[a] Reaction conditions: 15 mL stainless steel autoclave, glucose (1.00 mmol), acetylacetone (1.20 mmol), methanol (1.50 mL), alkaline earth metallic oxide (0.90 mmol), reaction temperature (70 °C), reaction time (2.0 h). Alkaline earth metal oxides were calcinated in nitrogen flow of 20 mL·min^{-1} at 350 °C for 2.0 h. The quantitative analysis was based on the standard curve method of HPLC. [b] Reaction time (4.0 h). [c] Commercial BaO was calcinated in static air atmosphere at 350 °C for 2.0 h.

Commercial alkaline earth metal oxides were utilized to promote the condensation reaction of glucose and acetylacetone. As shown in Table S2, the alkaline earth metal oxides were activated at 350 °C under nitrogen flow for 2.0 h to remove adsorbed water and other impurities. Glucose did not react with acetylacetone at 70 °C without base and could be recovered completely (Entry 1). As

MgO was used, the conversion of glucose was only 13.4%, and the target product, 4,8-anhydro-1,3-dideoxy-D-glycerol-D-gulo-2-nonulose, was not detected (Entry 2). The conversion of glucose significantly increased to 93.0%, and the yield of *C*-glucoside ketone was 30.4% as using CaO (Entry 3). Complete conversion of glucose accomplished with a yield of 36.1% of the target product was achieved as BaO utilized (Entry 4). The above results show that the conversion of glucose follows the order of MgO < CaO < BaO, which was consistent with the order of unit surface area basicity amount. Considering the relatively better performance of BaO, the reaction time was extended from 2 hours to 4 hours and the yield of *C*-glucoside ketone just increased from 36.1% to 39.8% (Entry 5). It was speculated that further extending the reaction time would not improve the reaction result. Therefore, the process of heat treatment was tuned to modulate the catalytic activity. Remarkably, the yield of the *C*-glucoside ketone increased to 77.0% promoted by BaO calcinated in static air atmosphere at 350 oC for 2.0 h (Entry 6).

5. Effect of solvent on the condensation reaction of glucose and acetylacetone
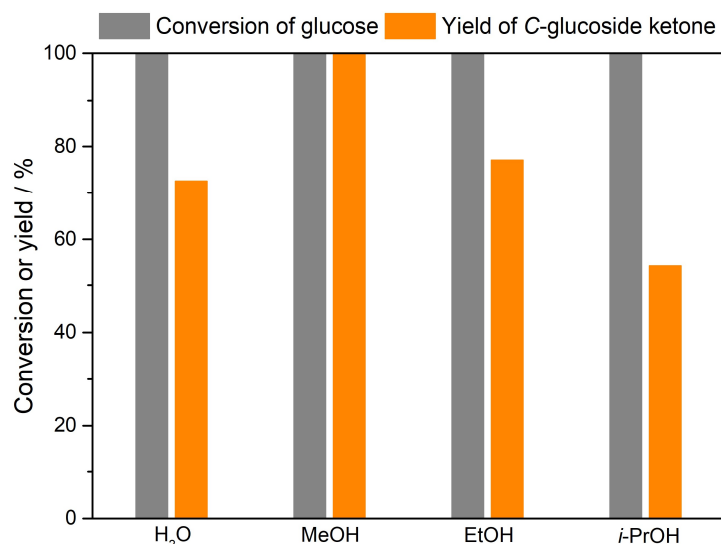
Fig. S3 Effect of solvent on the condensation reaction of glucose and acetylacetone. Reaction condition: 15 mL stainless steel reactor, glucose (1.00 mmol), acetylacetone (1.20 mmol), BaO (0.90 mmol), solvent (1.50 mL), reaction temperature (70 ºC), reaction time (3 h). Commercial BaO was calcinated under static air atmosphere at 350 ºC for 4.5 h. The quantitative analysis was based on HPLC.

6. Comparison of traditional inorganic base and calcinated BaO under air atmosphere
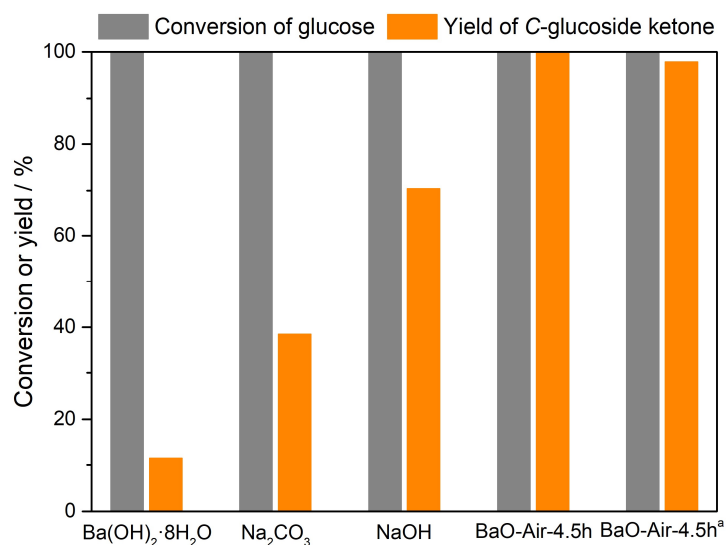

Fig. S4 Comparison of traditional inorganic base and BaO with calcination treatment under air atmosphere for the condensation reaction of glucose and acetylacetone. Reaction condition: 15 mL stainless steel reactor, glucose (1.00 mmol), acetylacetone (1.20 mmol), base (0.90 mmol), methanol (1.50 mL), reaction temperature (70 °C), reaction time (3 h). [a] 100 mL stainless steel reactor, glucose (10.00 mmol), acetylacetone (12.00 mmol), BaO (9.00 mmol), methanol (15 mL), reaction temperature (70 °C), reaction time (3 h). Commercial BaO was calcinated under static air atmosphere at 350 °C for 4.5 h. The quantitative analysis was based on HPLC.

7. NMR quantitative method to analyze the reaction results of various saccharides

The detailed procedure of NMR quantitative analysis was described as follows: The reaction mixture was added into 1 mL of deionized water to dissolve the unreacted saccharide substrate completely, and then shaken, sonicated, and the reaction solution was filtered to separate the catalyst. The filtrate was transferred into a 10 mL volumetric flask, diluted to volume and mixed. 2 ml of the above solution was transferred to a pear-shaped flask with a pipette, evaporated by rotation and concentrated to remove the solvent. Then 10 mg of maleic acid was weighed accurately and added to the pear-shaped flask as the internal standard. The resulting mixture was redissolved with deuterium oxide (D_2O) and analyzed by ^{1}H NMR to determine the yield of *C*-glycoside ketones.

The typical ^{1}H NMR spectrum for the quantitative analysis was showed in Fig. S5. Taking the reaction of mannose as a substrate for example, the two groups of split peaks at chemical shifts of 2.97-2.90 ppm and 2.82-2.77 ppm were the characteristic signals for the two protons of methylene (CH_2) of mannose. The peak at chemical shift of 6.31 ppm was assigned to the characteristic signal for two protons of carbon-carbon double bond of internal standard maleic acid. The peaks at 4.83 ppm and 3.35 ppm were assigned to the characteristic peaks of the residual water and methanol, respectively. The peak at 2.04 ppm was the characteristic peak of methyl (-CH_3) in acetic acid.
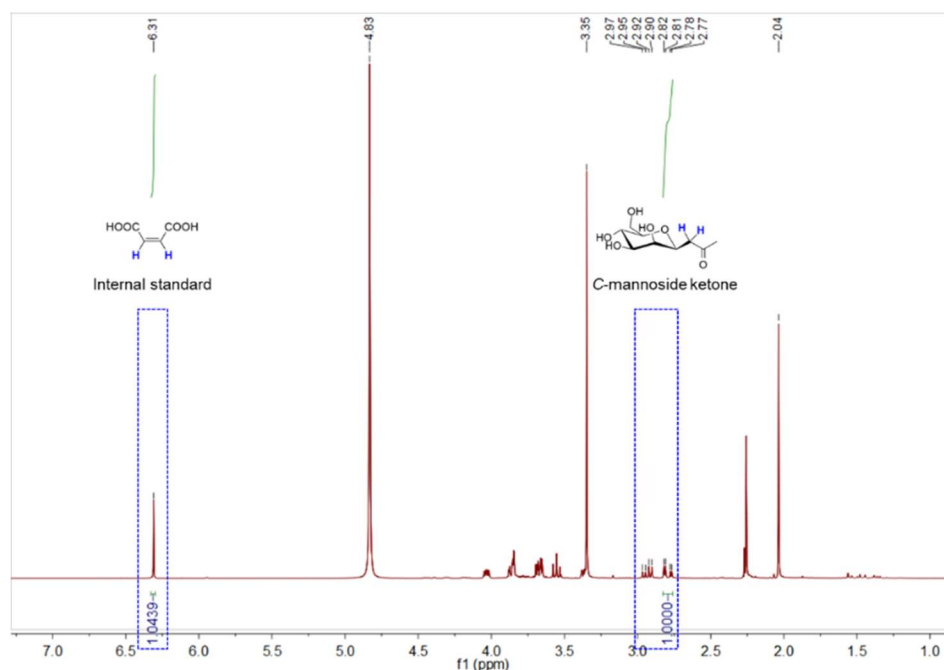
Fig. S5 Typical ^{1}H NMR spectrum for the quantitative analysis

The amount of C-glycoside ketone produced could be calculated by the following formulas.

$$W_x = W_s \times \frac{A_x}{A_s} \times \frac{E_x}{E_s}$$

W_x and W_s represent the mass of C-glycoside ketone produced and internal standard (maleic acid), respectively. A_x and A_s are the peak areas of characteristic proton of C-glycoside ketone and maleic acid (6.31 ppm, 2H). The definition of E_x is the proton equivalent of C-glycoside ketone at the characteristic chemical shift and the value is obtained by dividing the molecular weight of the sample by the number of protons at this characteristic chemical shift. The definition of E_s is the proton equivalent of maleic acid at the characteristic chemical shift of 6.31 ppm and the value is obtained by dividing the molecular weight (MW 116.07) by the number of protons at this characteristic chemical shift (6.31 ppm, 2H).

Table S3 Condensation reaction of various saccharides with acetylacetone catalysed by the calcinated BaO under static air atmosphere [a]

| Entry	Saccharide carbohydrate	C-glycoside ketone	Yield (%)
1	D-Glucose		>99.9
2	D-Mannose		99.7
3	D-Galactose		99.5
4	D-Xylose		>99.9
5	D-Maltose monohydrate		98.5

[a] Reaction conditions: 15 mL stainless steel reactor, saccharide (1.00 mmol), acetylacetone (1.20 mmol), BaO (0.90 mmol), methanol (1.5 mL), reaction temperature (70 °C), reaction time (4 h). The sample of BaO

was calcinated under static air atmosphere at 350 °C for 4.5 h. The quantitative analysis was based on ^{1}H NMR with maleic acid as an internal standard.
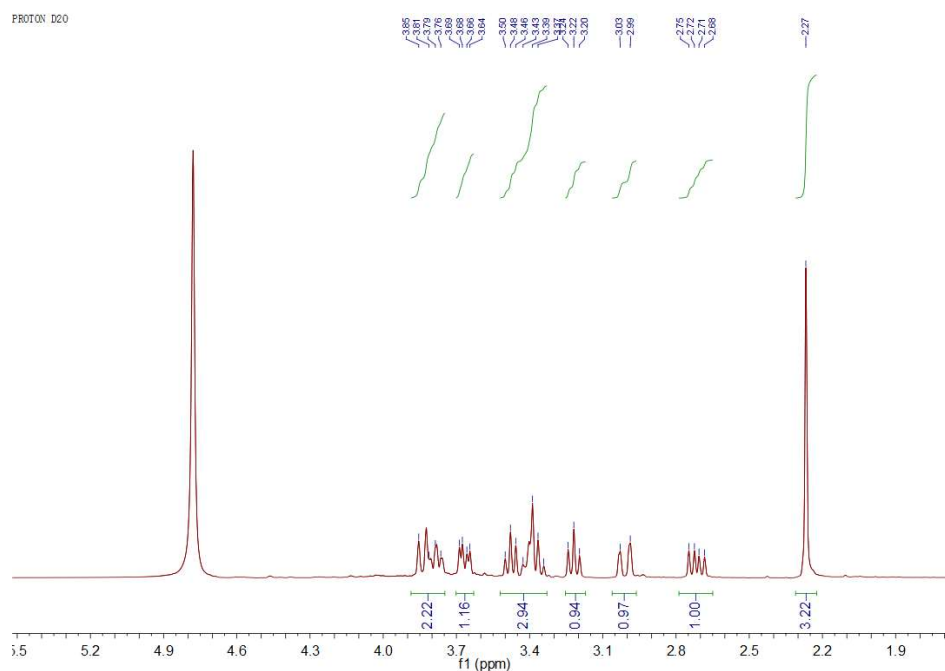
Fig. S6 ^{1}H NMR spectrum of 4,8-anhydro-1,3-dideoxy-D-glycerol-D-gulo-2-nonulose (*C*-glucoside ketone)
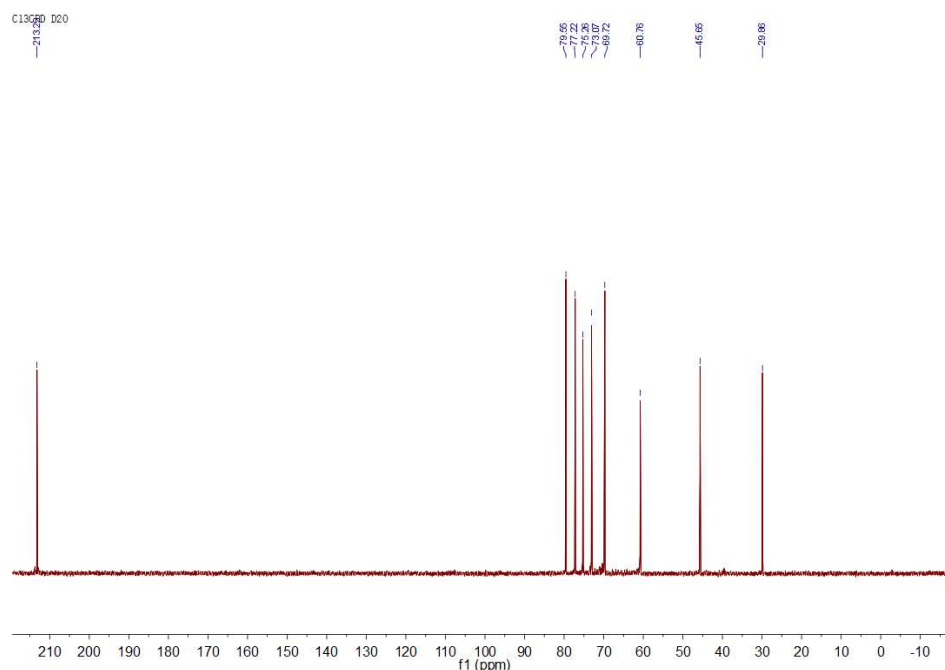
Fig. S7 ^{13}C NMR spectrum of 4,8-anhydro-1,3-dideoxy-D-glycerol-D-gulo-2-nonulose (*C*-glucoside ketone)

## 8. Absorption energy of reaction substrate on BaO₂ crystal facet provided by DFT calculation

All the calculations were carried out by the Vienna Ab-initio Simulation Package (VASP).[3,4] The Perdew-Burke-Ernzerhof (PBE) exchange-correlation functional with Grimme's zero-damping D3

correction was used.[5,6] The projector augmented-wave pseudopotential method was adopted, and the cutoff energy of the plane-wave basis was set to be 400 eV. Four-atomic-layer slab models with the bottom two layers fixed consisting of 64 Ba and 128 O atoms were built. The vacuum spaces were set as 15 Å between the layers. A gamma k-point sampling of 1×1×1 was selected. The convergences of energy and force were set to be 1×10^{-6} eV and 0.02 eV/Å, respectively.

Table S4 Absorption energy (eV) of mannose and acetylacetone on different crystal facets of BaO_2
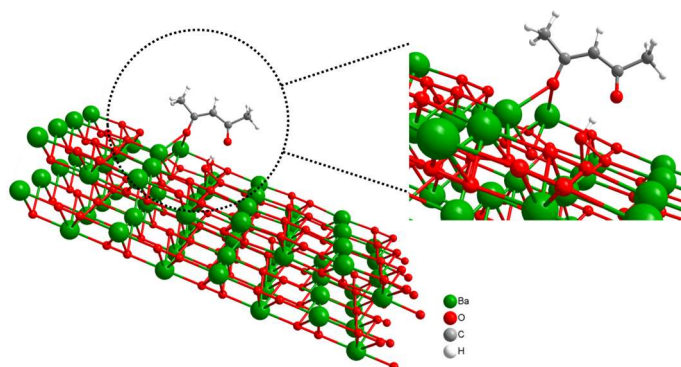
Entry	Reactant	Absorption energy on crystal facet of BaO_2 (ev)	
		(110)	(002)
1	Mannose	-1.62	-2.31
2	Acetylacetone	-1.48	-2.11
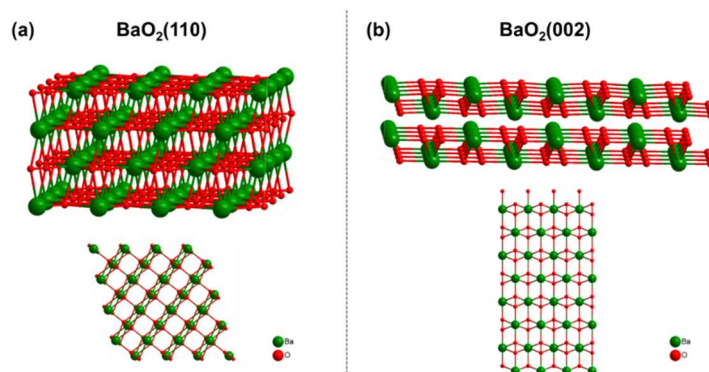
Fig. S8 Models for the crystal facets of BaO_2(110) and BaO_2(002)
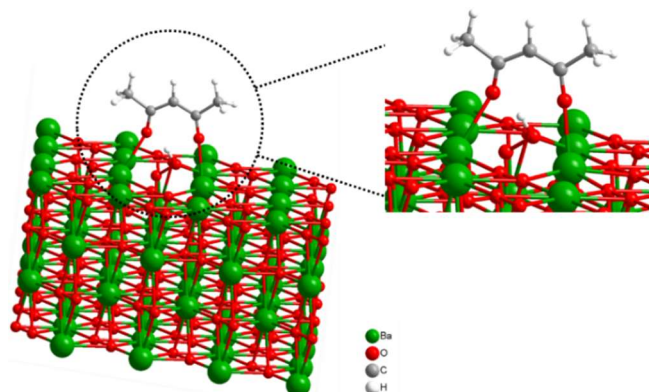
Fig. S9 Model for adsorption of acetylacetone on the crystal facet of BaO_2(110)

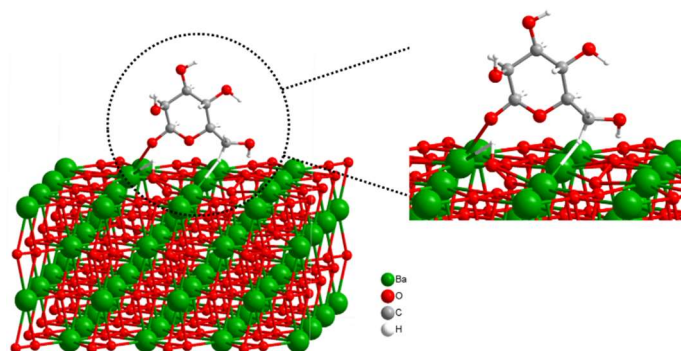**Fig. S10** Model for adsorption of acetylacetone on the crystal facet of BaO_2(002)

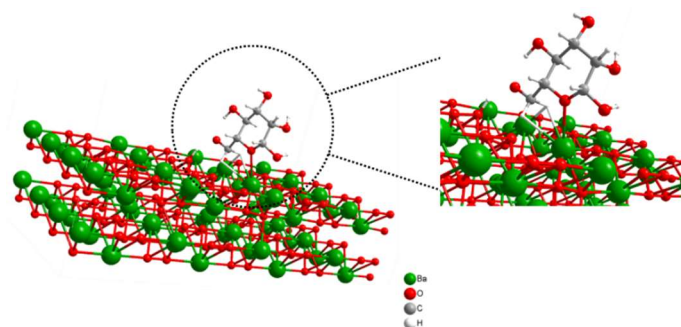**Fig. S11** Model for adsorption of mannose on the crystal facet of $BaO_2(110)$

Fig. S12 Model for adsorption of mannose on the crystal facet of $BaO_2(002)$

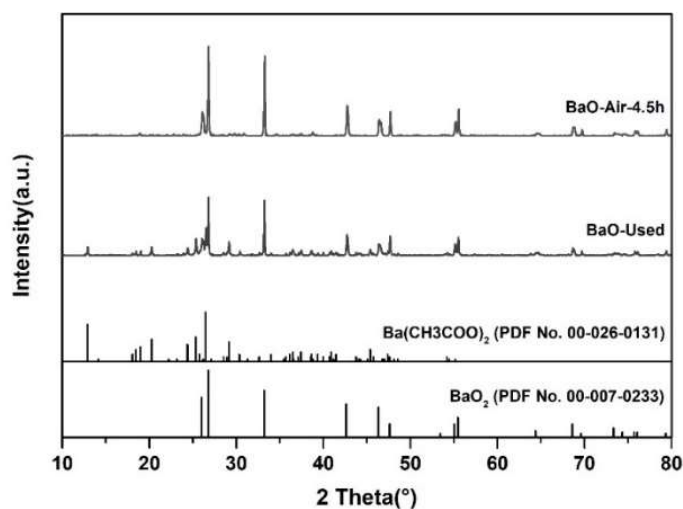## 9. XRD analysis of the used catalyst sample

Fig. S13 XRD profiles of the fresh BaO calcinated under static air and used sample

The calcinated BaO under static air atmosphere was used to promote the condensation reaction and then the solid sample was filtered, washed with methanol to remove adsorbed organics, and dried at 110 °C under vacuum before XRD analysis. The corresponding results were shown in Fig. S11 and the characteristic diffraction peaks of $Ba(CH_3COO)_2$ were detected except for that of BaO_2. This implied that BaO_2 might combine with the generated acetic acid to form $Ba(CH_3COO)_2$ during the reaction.

10. References

1   Y. Ono, H. Hattori, Solid Base Catalysis, in: A. W. Castleman Jr., J. P. Toennies, K. Yamanouchi W. Zinth (Eds.), *Springer Series in Chemical Physics*, Springer Berlin, Heidelberg, 2011.

2   S. Zhang, Y. Wei, S. Yin, C.-T. Au, Solid sodium stannate as a high-efficiency superbase catalyst for anti-Markovnikov hydroamination and hydroalkoxylation of electron-deficient olefins under mild conditions, *Catal. Commun.*, 2011, **12**, 712-716.

3   G. Kresse, J. Hafner, Ab initio molecular dynamics for open-shell transition metals, *J. Phys. Rev. B*, 1993, **48**, 13115-13118.

4   G. Kresse and J. Furthmüller, Efficient iterative schemes for ab initio total-energy calculations using a plane-wave basis set, *J. Phys. Rev. B*, 1996, **54**, 11169-11186.

5   J. P. Perdew, K. Burke, M. Ernzerhof, Generalized gradient approximation made simple, *Phys. Rev. Lett.*, 1996, **77**, 3865-3868.

6   S. Grimme, J. Antony, S. Ehrlich, H. Krieg, A consistent and accurate ab initio parametrization of density functional dispersion correction (DFT-D) for the 94 elements H-Pu, *J. Chem. Phys.*, 2010, **132**, 154104-154119.